Low-Noise Receiver Design Trends Using State-of-the-Art Building Blocks

HERMAN C. OKEAN, FELLOW, IEEE, AND ALEXANDER J. KELLY, SENIOR MEMBER, IEEE

Invited Paper

Abstract—**The current state-of-the-art and the various design tradeoffs encompassing the variety of low-noise microwave and millimeter-wave receiver "building blocks" which have evolved during the past two decades are described. Key examples of these are the high-idler noncryogenic parametric amplifier, the gallium arsenide field-effect transistor (GaAs FET) amplifier, and the image-enhanced Schottky-diode mixer.**

It is then shown how this inventory of building blocks can best be integrated into optimum receiver configurations for application in a multiplicity of future and present microwave and millimeter-wave communications, radar, and radiometer systems.

I. Introduction

THE low-noise receiver has evolved as the essential element in defining the performance level of a variety of microwave and millimeter-wave systems applications. Generically, the low-noise receiver "front end" consists of one or more stages of low-noise microwave or millimeter-wave amplification followed by a heterodyne frequency converter, the latter translating the received signals to the appropriate frequency range for signal processing. In the last two decades, a variety of "building blocks" for low-noise front ends have evolved in the direction of lower noise performance, solid-state implementation, smaller size, lighter weight, and longer life maintenance-free operation. Some of these, such as the maser, the low-noise traveling-wave tube, and the tunnel diode amplifier are diminishing in importance and currently experience at best limited usage, whereas others such as the high-idler noncryogenic parametric amplifier, the gallium arsenide field-effect transistor (GaAs FET) amplifier, and the image-enhanced Schottky-diode mixer are the primary constituents of current and future front ends.

Improvements in the noise performance of the receiver front end have resulted in corresponding improvements in the performance of microwave and millimeter-wave communications, radar, and radiometer systems, by virtue of greater communications predetection signal-to-noise ratio, increased radar range or reduced radar transmitter power, and decreased radiometer minimum detectable temperature, respectively. It is the purpose of this paper to assess the state-of-the-art in the various low-noise front-end building blocks and to show how this inventory of building blocks can be best integrated into optimum receiver configurations tailored to each of the foregoing systems applications.

Manuscript received September 15, 1976; revised September 30, 1976. Some of the equipment described in this paper was developed under sponsorship of the NASA Goddard Space Flight Center, Greenbelt, MD; Air Force Avionics Laboratory, Dayton, OH; Naval Electronics Laboratory Center, San Diego, CA; Naval Air Systems Command, Washington, DC; and Rome Air Development Center, Rome, NY.

The authors are with the Department of Research and Development, LNR Communications, Inc., Hauppauge, NY 11787.

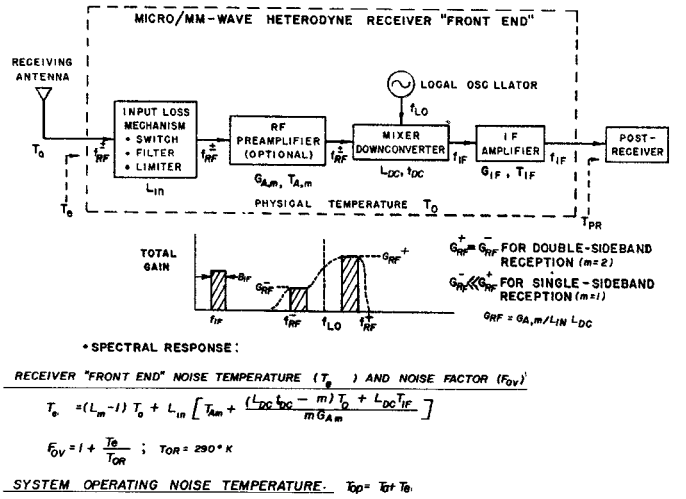

Fig. 1. Block diagram of generic single-channel heterodyne front end.

II. Description of General Receiver Front End

A. Functional Description

A generic single-channel low-noise receiver front end, pertinent to each of the microwave/millimeter-wave systems applications under consideration, is of the heterodyne type in which one or both RF input sidebands are translated via a single downconversion, into a single IF band. Depicted in block diagram form in Fig. 1, this generic front end consists of the following:

—Input coupling network forming interface between receiving antenna feed and subsequent front-end components, and providing filtering, switching, limiting, and/or test signal injection functions, depending upon particular receiver application.

—Single or multistage RF amplifier centered at microwave or millimeter-wave carrier frequency and, in the latter case, often representable as the cascade of an ultra-low-noise RF preamplifier and a moderately low-noise high dynamic range RF postamplifier.

—Frequency downconverter, including input power divider or demultiplexer loss, resistive mixer with self-contained or externally provided local oscillator (LO) and

IF amplifier, centered at a convenient IF range for demodulation, processing, further downconversion, etc., depending upon the system application.

All succeeding circuits providing the foregoing further downconversion, processing, and/or demodulation functions as well as possible further demultiplexing and/or power division, and in aggregate comprising the postreceiver, are not considered part of the front end under consideration and are not within the province of this discussion (assuming sufficient total front-end RF/IF gain to offset any significant postreceiver contributions to overall receiver noise performance). Furthermore, the most general low-noise front end can consist of a multiplicity of RF amplifier/downconverter channels demultiplexed off a common receiving antenna feed or of many RF downconverter channels demultiplexed off a common RF amplifier. However, each individual RF/IF input/output path or "channel" is representable by the generic single-channel block diagram of Fig. 1.

Within the context of Fig. 1, most microwave and millimeter-wave front ends utilize either *single-* or *double-*sideband heterodyne reception, in which input frequencies $f_{RF}^{\pm} = f_{LO} \pm f_{IF}$, situated in *one* or *both* sidebands of the downconverter LO frequency f_{LO} are translated down to the IF (f_{IF}), with overall conversion gains $G_{0v}^{\pm}$, respectively. In the majority of receiving systems applications, including communications and telemetry links, coherent radar and electronic warfare, discrete information-bearing signals in one input sideband must be received and processed unambiguously with respect to extraneous signals in the other "image" or unwanted sideband.

Therefore, in single-sideband (SSB) front ends, a high degree of rejection is generally presented to the unwanted image sideband by the selectivity of the RF preamplifier by the presence of a "preselector" bandpass filter preceding the mixer and/or by the use of a mixer configuration with inherent image rejection properties ($G_{0v}^{-} \ll G_{0v}^{+}$).

In contrast to the aforementioned, there are other receiving system applications including radio astronomy, radiometry, and noncoherent radar, in which the received signal is broad-band noise appearing in both input sidebands. In these cases, sensitivity is maximized by the use of a double-sideband (DSB) receiver ($G_{0v}^{+} \approx G_{0v}^{-}$).

B. General Formulation of Front-End Noise Performance

The noise performance of the generic heterodyne front end (Figs. 1 and 2) is formulated [1], [2] in terms of that of each of its constituent building blocks in Fig. 1, as characterized by the familiar parameters, broad-band input noise temperature (T_e), and noise factor (F). These formulations make use of the foregoing assumptions on $G_{0v}^{\pm}$ for SSB and DSB reception.

A more meaningful measure of overall antenna/receiver system sensitivity relevant to the aforementioned microwave/millimeter-wave applications is *system operating noise temperature* T_{op}, which in turn is expressible [1], [2]

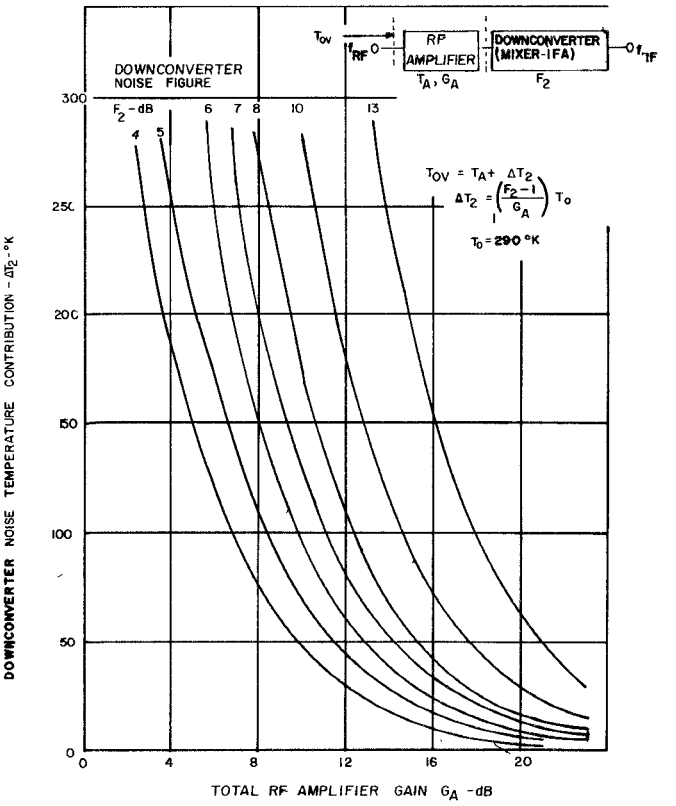

Fig. 2. Downconverter contribution to overall front-end noise temperature.

in terms of T_e and antenna temperature T_a as indicated in Fig. 1.

It is immediately clear from Fig. 1 that for antenna temperature T_a equal to T_{OR} = 290 K (as is often the case), system operating noise temperature and receiver noise figure are very simply related by

$$F = T_{op}/T_{OR}. \tag{1}$$

The equivalent antenna temperature T_a is a strong function of antenna orientation relative to the earth, antenna elevation, and received signal frequency [3] with the following particular cases applicable to the majority of microwave and millimeter-wave system applications:

—Ground-based antenna, vertical elevation pointing at "cold" sky (satellite communications, space telemetry radar, radio astronomy): $T_a < 10$ K and T_a = 15–75 K for frequency between 1 and 20 GHz and 20 and 100 GHz, respectively (except for absorption region between 50 and 60 GHz, for which T_a = 290 K).

—Ground-based antenna, horizontal elevation (radar, point-to-point communications): T_a = 125–250 K over 1–100 GHz, and about 290 K at or above 20 GHz.

—Airborne, ground-looking antenna (radar, radiometric mapping, communications): T_a = 300 K over 1–100 GHz.

In any given microwave and millimeter-wave system application, the optimum tradeoff between sensitivity and system cost and complexity occurs at a level of receiver noise performance (T_e) compatible with antenna tem-

perature, e.g., $T_e \sim T_a$. Therefore, in light of the preceding, it is seen that certain systems applications (satellite communications links, space research, radio astronomy) require the ultimate in receiver noise performance ($T_e \lesssim 50$ K) whereas others can effectively utilize moderately low-noise performance ($T_e \approx 300$–1000 K). This, in turn, impacts the choice of receiver front-end configuration for a given application, as will be discussed in a subsequent section of this paper.

The foregoing formulations of overall front-end noise performance underscore the importance of minimizing total functional (duplexer, limiter, switch, filter, etc.) input circuit losses (L_{in}). Hence $1.05 \leq L_{in} \leq 1.25$ (0.25–1 dB) in most representative system applications. Even more importantly, they emphasize the role of and frequent necessity for low-noise RF preamplification, with sufficient RF preamplifier gain (G_A) provided to minimize contributions of the downconverter (and possibly of the RF postamplifier immediately preceding it) to overall receiver noise figure, so that the noise figure of the RF amplifier defines that of the front end.

This introduces an important tradeoff in overall front-end design, that is, downconverter noise performance versus required RF amplifier gain for a given degree of downconverter noise contribution suppression. This tradeoff is exemplified in Fig. 2, which depicts the second-stage noise temperature contribution ΔT_2 as a function of second-stage noise figure and RF amplifier gain. Fig. 2 provides the rationale for some of the specific front-end alternatives such as dedicated low-noise downconverter and single-stage low-noise RF amplifier versus demultiplexed multichannel downconverter and multistage low-noise RF amplifier or single-stage low-noise RF preamplifier plus moderate noise RF postamplifiers, as will be described in subsequent sections of this paper.

C. Other Aspects of Low-Noise Receiver Performance

In addition to noise performance, other important receiver front-end parameters include RF/IF bandwidth and dynamic range.

The RF input bandwidth (B_{RF}) of the generic heterodyne receiver front end is related to the output IF bandwidth (B_{IF}), as a function of the particular mode of mixer operation under consideration (Fig. 1), with the majority of cases encompassing the following:

—Tunable LO, broad-band image mixer with overlapping signal, LO, and image bands. Suitable for either DSB or SSB reception, the latter requiring the use of properly phased dual mixers for image rejection and possible image enhancement ($B_{RF} \gg B_{IF}$, $B_{IF} \approx 30$–200 MHz).

—Fixed LO, broad-band image mixer with separate signal and image sidebands. Suitable for either DSB or SSB reception, the latter requiring a fixed preselector isolator at the input for image rejection under matched-image termination ($B_{IF} = B_{RF}$ SSB and B_{RF} DSB $= 2f_{IF}{}^{+} > 2B_{IF}$).

—Fixed LO, reactive image-enhanced SSB mixer with properly situated preselector at RF input to provide optimum reactive termination to mixer diodes over image band for minimum SSB conversion loss, while simultaneously providing high image rejection ($B_{RF} = B_{IF}$).

Typically, microwave and millimeter-wave heterodyne front ends utilizing tunable LO operation can be configured with RF bandwidths of an octave or more, but those operating as SSB or folded DSB translators exhibit maximum RF bandwidths of 5–20 percent. In each case, the front-end RF bandwidth capability is determined by the specific type of building blocks employed therein, as described in a subsequent section.

The dynamic range of the generic microwave/millimeter-wave front end is characterized at the low end by noise performance and upper end by the onset of nonlinearity, as defined by one or more of the following generally interrelated [4] parameters, depending upon the specific system application:

—Deviation from input/output linearity exemplified by input or output level at which 1-dB gain compression occurs.

—Two-tone third-order intermodulation (IM) intercept point, referenced to input or output (P_{inIM},P_{oIM}) representing an extrapolation of the levels of the two IM products (at frequencies $2f_1 - f_2$ and $2f_2 - f_1$) generated by two equal in-band tones at f_1 and f_2 to the point where tones and IM products become equal.

—AM-to-PM conversion coefficient defined by the degree of output phase distortion encountered over a 1-dB variation in input amplitude about some nominal level.

For the type of nonlinearities associated with most microwave and millimeter-wave amplification and conversion devices, the preceding parameters are precisely related to one another [4]. Therefore, the third-order output IM intercept point is customarily chosen as the nonlinearity parameter characterizing most microwave and millimeter-wave receivers and their constituent components. In fact, the output intercept point of the generic front ends (Fig. 1) can be expressed in terms of that of its key constituents, the RF amplifier, downconverter mixer, and IF amplifier, as given by [5]

$$P_{oIM_{ov}} = P_{oIM_{IF}} \left(1 + \frac{P_{oIM_{dc}} L_{dc}}{P_{oIM_A}} + \frac{P_{oIM_{IF}} L_{dc}}{G_{IF} P_{oIM_A}}\right)^{-1} \quad (2)$$

where

P_{oIM_A},$P_{oIM_{dc}}$,$P_{oIM_{IF}}$ third-order output intercept points of RF amplifier, mixer downconverter, and IF amplifier, respectively;

L_{dc},G_{IF} downconverter mixer conversion loss and IF amplifier gain.

The implication of the preceding relationship is that in many microwave and millimeter-wave front ends, particularly those employing high-gain IF amplifiers, it is the output IF amplifier dynamic range capability that defines that of the entire front end. Therefore, in many cases the RF amplifier for the generic front end can be of relatively modest large-signal capability. The impact of the

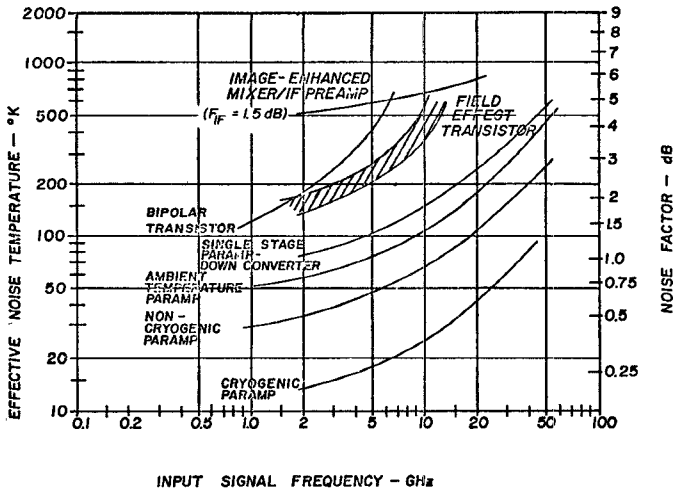

Fig. 3. Noise performance of state-of-the-art front-end building blocks.

preceding on the choice of front-end components will be described in a subsequent section.

III. State-of-the-Art Receiver Building Blocks

A. General Comparative State-of-the-Art

A variety of building blocks have evolved during the past two decades for use in low-noise microwave and millimeter-wave front ends. Some of these such as the traveling-wave maser and the low-noise linear traveling-wave tube amplifier see only limited usage and are being almost completely supplanted by solid-state amplifiers, such as the parametric amplifier, the bipolar and FET amplifier, and to a lesser extent, the tunnel diode amplifier. In addition, the original point-contact diode mixers have given way to sophisticated broad-band image and image-enhanced low-loss Schottky-diode (and more recently FET) mixers.

Fig. 3 summarizes the current state-of-the-art of receiver front-end performance [6]–[45] as a function of input signal frequency.

In the past few years significant progress has been made in translating laboratory results into reliable operational hardware. Much of this progress has been as a result of advances in semiconductor technology (particularly applied to varactor, mixer, Gunn diodes, and MESFET transistors; lower loss ferrite circulators and isolators; and new and maturing microwave circuit structures and design techniques).

From among the aforementioned building blocks, the most recent emphasis has been upon the following:

—Continually decreasing noise temperatures in non-cryogenic parametric amplifiers with noise temperatures as low as 30–90 K for frequencies from 2 to 15 GHz.

—Ultralow-noise parametric amplifiers in the 10–40-GHz region.

—High-reliability spacecraft-qualified miniature parametric amplifiers, operated at ambient or elevated temperatures.

—Low-noise FET's as front ends and as postamplifiers for paramps.

—Image-recovery mixers as low-noise front ends and as second stages for parametric amplifiers.

The aforementioned key building blocks are described in more detail in the following paragraphs.

B. Description of Individual Building Blocks

1) Parametric Amplifiers and Converters: The parametric amplification mechanism arising from the multiple-frequency interactions within a variable-capacitance varactor, pumped at f_p, has led to two extremely low-noise amplifier/converter configurations, depicted in block diagram form in Fig. 4. These configurations are as follows:

—The positive-resistance upper sideband upconverter (USUC), in which inputs at f_s are converted to sum-frequencies $f_u = f_p + f_s$, with gain $\leq (f_u/f_s)$.

—The circulator-coupled negative-resistance parametric amplifier in which negative resistance, generated at f_s under proper nominal short-circuited termination of the idler at $f_i = f_p - f_s$, is capable of unlimited reflection, but at the expense of bandwidth and operational gain stability. Two paramp configurations are possible: the nondegenerate (SSB) with $f_p = 2f_s$ and the degenerate (DSB) with $f_{i0} = f_{s0} = f_p/2$.

The paramp noise temperature cited in Fig. 3 are for SSB nondegenerate configuration, the corresponding DSB degenerate paramp noise temperature would be about 70 percent of that given.

The USUC is useful primarily over the UHF/*L*-band input frequency range (0.1–1.0 GHz) where sufficiently wide-band low-loss circulators are not always available. Circulator-coupled paramps, on the other hand, have been utilized from 1 to about 50 GHz and are feasible up to about 100 GHz. Therefore, for microwave and millimeter-wave applications, the remainder of this discussion will focus upon the circulator coupled negative resistance parametric amplifier.

The key design alternatives underlying the development of most current paramps [6]–[20] relate primarily to their impact on paramp noise performance and are enumerated as follows:

—Degenerate versus nondegenerate, depending on application as to whether DSB or SSB reception is required.

—Pump frequency (nondegenerate): The noise performance (and bandwidth capability) of a circulator-coupled paramp improve with increasing pump frequency up to a broad optimum value, beyond which degradation is encountered. The optimum pump frequency selection is further impacted by the realizeability of the required pump source in solid-state form.

—Varactor quality: The lower the varactor loss content (the higher the cutoff frequency) the lower the paramp noise temperature. However, this dependence is weak, particularly at low signal frequencies, where circuit rather than semiconductor losses predominate.

—Circulator implementation: Waveguide (lowest loss) versus stripline (more compact and wider band).

—Number of stages (gain per stage) (nondegenerate): Both gain bandwidth and operational stability considera-

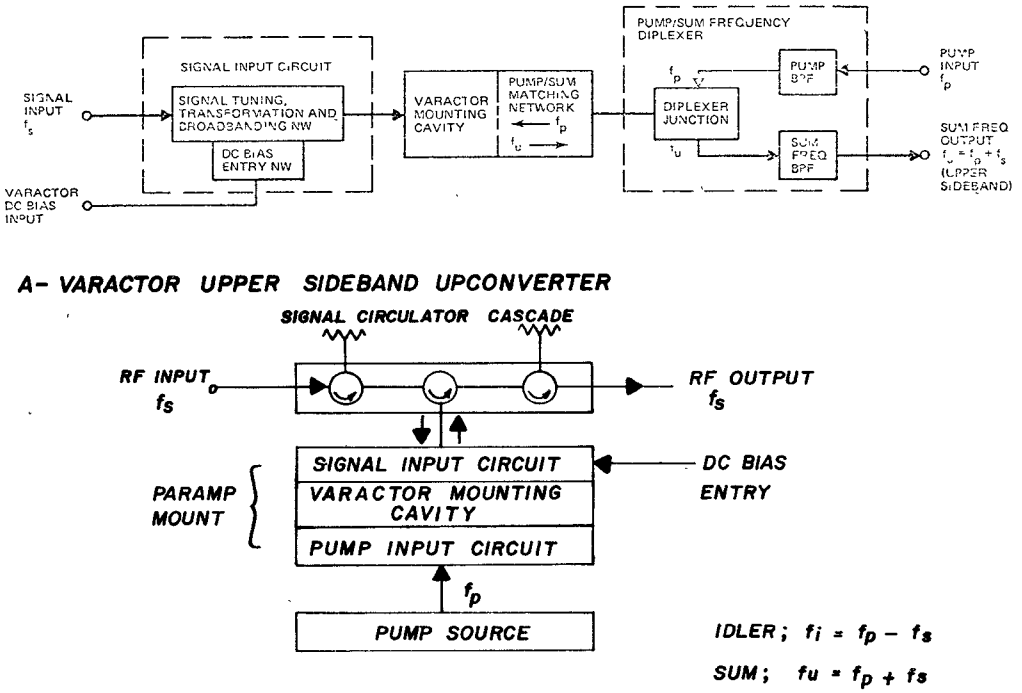

Fig. 4. Block diagram of parametric amplifier and upconverter.

tions dictate that paramp gain per stage be limited to 14 dB maximum for moderate to wide-band applications (greater than 10 percent fractional bandwidth) whereas somewhat higher passband gain levels (18-dB maximum) per stage be considered only for extremely narrow-band (less than 5 percent fractional bandwidth) applications.

—Physical temperature: Due to the absence of shot noise, the noise temperature of the parametric amplifier is directly related to its absolute operating temperature. Therefore, based upon the use of GaAs varactor technology, paramps have been readily operated at cryogenic (20 K), room ambient, or elevated (320 K) temperatures.

Within the context of the foregoing design alternatives, single and multistage parametric amplifiers have exhibited noise temperatures as low as 10–100 K over the entire microwave range and well into the millimeter-wave region, concurrently with bandwidth capability from 5 percent to almost half-octave and with output IM intercept points from −20 to 0 dBm. Particular examples of the current paramp art (Fig. 3) include the following.

a) Cryogenic Paramps: Refrigerated to 20 K and capable of virtually noise-free amplication (T_e = 10–50 K) over the microwave and much of the millimeter-wave [11] frequency range, these have essentially supplanted the maser for use in large satellite communications and radio astronomy ground stations, but are costly and require periodic maintenance of the closed cycle mechanical refrigerators.

b) Advanced Noncryogenic Paramps: Utilization of ultrahigh-quality low-parasitic-content GaAs varactors, solid-state millimeter-wave pump sources (f_p = 50–100 GHz), extremely low-loss stripline and waveguide ferrite circulators, and efficient thermoelectric (Peltier) cooling modules has resulted in noncryogenic ultralow-noise amplification with near cryogenic performance (T_e = 30–90 K) at frequencies from S to K_u band, with 5–15 percent bandwidths and in completely packaged RF amplifier assemblies consisting of dual-stage paramps and possibly transistor postamps, along with self-contained solid-state pump sources, Peltier modules, and dc power and control circuits. Examples of the preceding include the following:

i) Deployment of hundreds of RF amplifier assemblies consisting of dual-stage paramp/transistor postamplifiers and providing typical noise temperatures of 45 K in the 3.7–4.2-GHz common carrier band in communications satellite (3.7–4.2 GHz) earth stations throughout the world.

ii) Fully packaged and operational [12] K_u-band two-stage 26-dB-gain paramp (Fig. 5) demonstrating noise temperatures of 76–84 K over the 14.7–15.2-GHz NASA Downlink Band by virtue of the use of a solid-state 30-mW 96-GHz pump source comprising a 48-GHz Gunn oscillator driving a highly efficient varactor doubler, a single-pass high isolation waveguide circulator with a forward loss of 0.07 dB and a high-quality GaAs chip varactor in a single-ended raised idler configuration, forming the highest idler resonance (81 GHz) ever reported.

c) Single-Stage Paramp Assemblies: For less demanding low-noise requirements, coupled with stringent size, cost, and/or environmental constraints, a preferable composite RF amplifier configuration consists of a single-stage paramp followed by a moderately low-noise postamplifier, and incorporating self-contained pump sources, dc power regulation and thermal stabilization circuits, and operated at a slightly elevated temperature. As an example, a weather-proof assembly incorporating a single-stage 3.7–4.2-GHz paramp plus transistor postamplifier provided typical noise

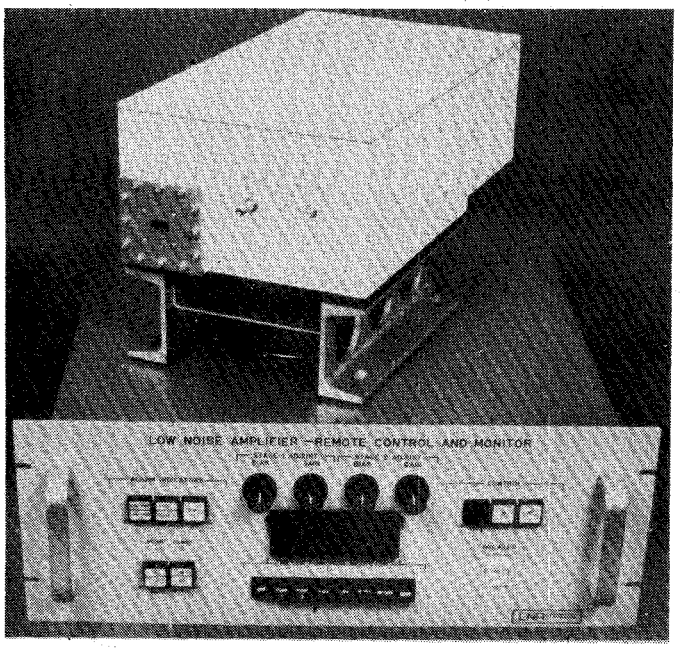

(a)

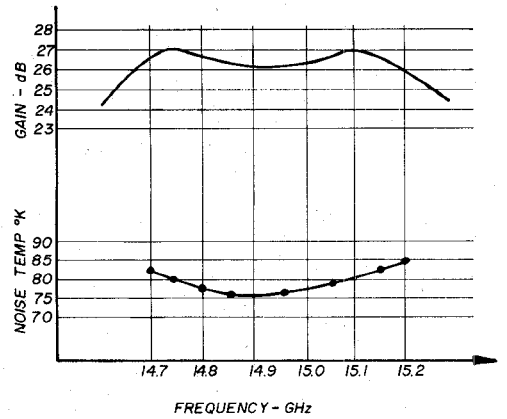

(b)

Fig. 5. Ultralow-noise noncryogenic parametric amplifier assembly. (a) Photograph. (b) Measured performance.

temperatures of 75–85 K when operated in small shipboard, oil rig, and unattended Alaska Bush earth terminals.

d) Spaceborne Paramps: Single-stage paramps addressing the stringent demands of space operation, with the attendant requirements on small size and weight, low power drain, immunity to severe shock and vibration, precise thermal stabilization, and ultralong life, are exemplified by the development for NASA of a fully operational spacecraft-qualified *S*-band low-noise parametric amplifier which is completely self-contained and requires less than 8 W of dc prime power. A gain of 18 dB, noise temperature of less than 45 K over the 2.2–2.3-GHz band (Fig. 6), were achieved in a 21-oz package which withstood severe vibration and shock and demonstrated operation in a vacuum environment. Other miniaturized single-stage paramps for space applications [13], [14] at frequencies as high as K_u band, exhibited noise temperatures as low as 150 K.

e) Millimeter-Wave Paramps: A K_a-band paramp assembly, developed [15] for satellite communications in the

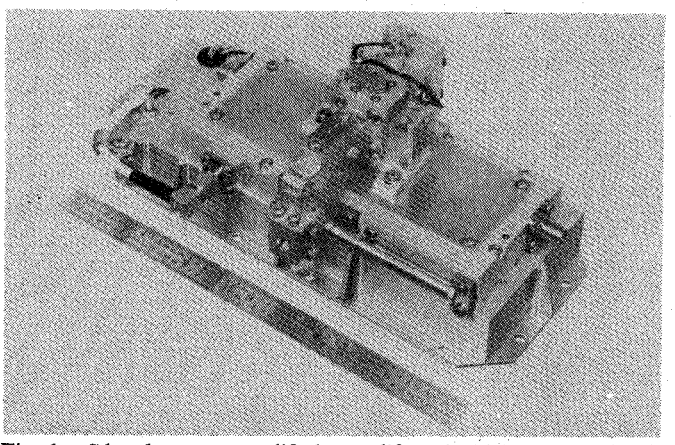

Fig. 6. *S*-band space qualified amplifier (NASA space shuttle prototype).

35–40-GHz low atmospheric attenuation window, and incorporating [Fig. 7(a)] a directly integrated 96-GHz Gunn oscillator/varactor tripler pump source and self-contained dc power regulation, control and elevated temperature thermal stabilization circuits for 0–60°C operation, is electronically tunable, covering 36.5–38.5 GHz, and has a noise temperature of 350 K. Under its intended bimodal operation, the paramp is switch-tuned upon external voltage command to either of two specific frequency slots separated by over 1 GHz, as shown in Fig. 7(b), each providing 15 $\pm$ 0.5-dB gain over an instantaneous bandwidth of 150 MHz. However, under broad-band alignment this K_a-band paramp exhibited [Fig. 7(b)] 14-dB minimum gain with 1000-MHz instantaneous bandwidth. In addition, a solid-state pumped single stage operating in the 55–65-GHz region has been demonstrated [16] with less than a 6-dB noise figure. Finally, the varactor, circulator, and circuit technology for a 94-GHz paramp has been developed [17], but realization of useful performance awaits development of a sufficiently high-power 170–200-GHz CW pump source.

An additional application of parametric amplifiers in millimeter-wave low-noise front ends is as microwave IF preamplifiers used in conjunction with low-loss millimeter-wave mixer downconverters. Of particular advantage in radio astronomy receivers [21], the use of an IF amplifier consisting of a moderate gain, 20 percent or greater bandwidth paramp stage followed by a transistor postamplifier can provide a 1–3-dB improvement in downconverter noise figure as compared with the use of an all-transistor IF amplifier. This approach is especially advantageous at cryogenic temperatures, utilizing cryogenic mixer and paramp technology [22].

2) Paramp/Downconverter Assemblies: A logical extension of the completely packaged self-contained parametric RF amplifier assemblies described previously is the integration of an uncooled single-stage paramp and a low-loss (possibly image-enhanced) mixer/downconverter/transistor IF amplifier (and associated power, control, and thermal stabilization circuits) in a single self-contained enclosure (with or without a self-contained LO for the mixer) which is compact and light enough for antenna

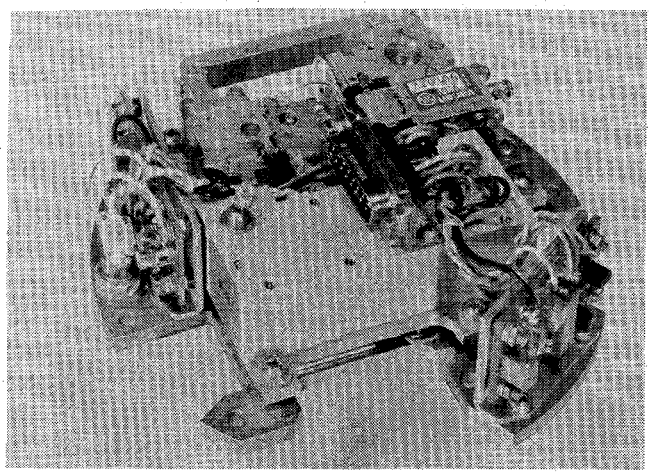

(a)

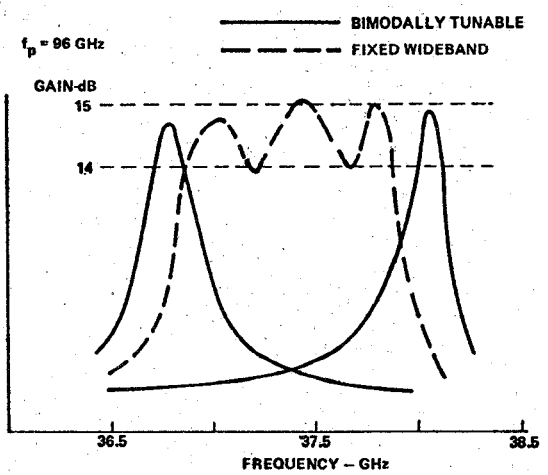

(b)

Fig. 7. Miniature K_a-band paramp assembly. (a) Photograph. (b) Measured gain response.

mounting. Such units, of particular use at high microwave and millimeter-wave input frequencies (7–42 GHz) at which low-noise transistor RF postamplifiers are either not always cost-effective (7–12 GHz), or do not exist (12–42 GHz), are available as operational hardware in the 7.25–7.75-GHz military communications and 11.7–12.2-GHz communications technology satellite (CTS) bands (Fig. 8), exhibiting overall noise temperatures (with 1-GHz IF) of 115 and 220 K, respectively, and usable with IF's from 70 MHz to 2 GHz.

A similar single-stage paramp/downconverter configuration has been implemented for shipboard satellite communications receiver usage in the 35–40-GHz range [15]. Utilizing the previously described "bimodally" tunable K_a-band paramp design, and incorporating a balanced GaAs Schottky-diode mixer and a low-noise UHF transistor amplifier [34], this low-noise front end exhibits an overall SSB noise factor of less than 4 dB, an overall conversion gain of 34 $\pm$ 1 dB, and an instantaneous RF/IF bandwidth of 150 MHz, which is bimodally switch-tunable to either sideband of the externally provided 37.5-GHz LO. The overall paramp/downconverter enclosure, including dc

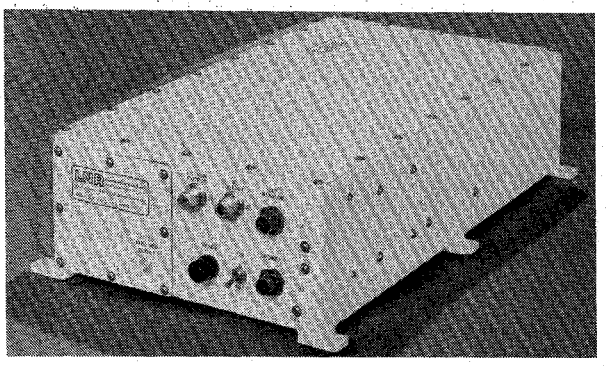

Fig. 8. Low-noise 11.7–12.2-GHz integrated parametric amplifier downconverter.

power supply and thermal stabilization, measures only 6 × 5 × 4 in.

3) Transistor Amplifiers: Transistor amplifiers find application in the generic heterodyne front ends under consideration (Fig. 1) at frequencies from VHF to K_u band either as RF or IF amplifiers.

Significant recent advances [6]–[10], [23]–[26] in the realization of low-noise GaAs FET and Si bipolar transistor amplifiers has yielded, in the state-of-the-art limit, superior noise performance (T_e = 75–600 K, F = 1–5 dB) to all but the paramp and maser, at frequencies up to about 15 GHz, with Si bipolars providing lower noise performance through lower S band and GaAs FET's having the edge above 3 GHz. These advances have been achieved primarily on the strength of refinements in Si and GaAs device processing, resulting in smaller electrode geometries, reduced parasitics, and consequently higher maximum frequencies of operation. In GaAs FET devices, unlike bipolars, shot noise does not completely dominate, and the thermal noise contribution is more significant, so that potential noise figure improvement at reduced physical temperatures is a reality.

Current state-of-the-art in bipolar and GaAs FET amplifier production hardware is summarized as follows [6]–[10], [23]–[26]:

Frequency	Bandwidth	Device	Geometry	Maximum Noise Figure
VHF/UHF	octave	bipolar	—	1.5 dB
2 GHz	< 20 percent	bipolar	—	2.5 dB
4 GHz	< 20 percent	bipolar	—	3.5 dB
1–2 GHz	octave	bipolar	—	3 dB
2–4 GHz	octave	bipolar	—	4 dB
3.95 GHz	500 MHz	GaAs FET	1-μm gate	2.5 dB (uncooled)
3.95 GHz	500 MHz	GaAs FET	1-μm gate	1.8 dB (cooled to −40°C)
4 GHz	2 GHz	GaAs FET	1-μm gate	4.5 dB (uncooled)
8 GHz	1.2 GHz	GaAs FET	1-μm gate	5–6 dB (uncooled)
12 GHz	1.2 GHz	GaAs FET	1-μm gate	5.5 dB
12 GHz	—	GaAs FET	1-μm gate	1.2 dB (cooled to 40 K)
14 GHz	500 MHz	GaAs FET	0.5-μm gate	5 dB (uncooled)
15 GHz	6 GHz	GaAs FET	0.5-μm gate	5–6.5 dB

The preceding results are obtained in multistage configurations with typical gain per stage decreasing from 12 to 6 dB from VHF to K_u band and with output IM intercept points above +10 dBm. Construction is typically in stripline or coax at UHF and the lower microwave frequencies where various encapsulated device form factors predominate, but is almost exclusively microstrip above C band, for maximum compatibility with the unencapsulated device embedding necessary for optimum performance. Input and output matching is accomplished by a combination of reciprocal lossless network techniques, use of ferrite isolators at input and/or output, and implementation of the balanced configuration [26] in which a pair of identical amplifiers are coupled through the in phase and quadrature parts of 0–90° 3-dB hybrids to the input and output interfaces.

It is expected that the further refinement of 0.5-μm Schottky-barrier MESFET gate geometry will result in even further reduction in GaAs FET amplifier noise figure and in extension of the maximum usable frequency range to beyond 20 GHz. Concurrent improvements in GaAs FET processing technology should eliminate any remaining questions on device operational stability and reliability.

4) Tunnel Diode Amplifiers: The tunnel diode amplifier (TDA) is a negative-resistance amplifier (by virtue of the negative-slope region in its dc current–voltage characteristic) usually operated in the circulator-coupled-reflection mode [2], [6], [27]. Its primary noise mechanism is that of shot noise due to dc current flow through the degenerate p-n tunnel diode junction, so that there is negligible advantage in below-room-temperature operation.

Shot-noise constant N and, hence, overall TDA noise temperature T_A $300N$, are primarily functions of the semiconductor material comprising the tunnel diode. For the three commonly used materials (GaSb, Ge, GaAs), the shot-noise constants N are approximately 0.8, 1.2, and 2.0, respectively. Hence GaSb tunnel diodes yield lowest noise operation, followed by Ge and GaAs diodes. (The reverse is true for RF saturation capability; therefore, Ge tunnel diodes are generally chosen as the best compromise between low noise and high saturation.) GaSb diodes are also difficult to manufacture and hence find very limited usage.

Since the noise performance of TDA's is essentially limited by the constants of the diode semiconductor material, little future improvement therein is anticipated. Despite the extreme simplicity, low power drain, and half to full octave bandwidth capability of the TDA, its current role [2], [6] as a moderately low-noise (F = 4.0–7.0 dB from 2 to 25 GHz) RF amplifier is being steadily supplanted by the low-noise bipolar transistor and FET RF amplifier below K_u band, and, in the millimeter region, by the low-conversion-loss image-enhanced mixer without RF preamplification, by virtue of both the significant improvements in noise performance of the latter two components and the limited dynamic range capability of the TDA (IM intercept point: −30 to −10 dBm). In addition, TDA's are being replaced by reduced-cost miniaturized paramps in certain applications (e.g., radar receivers) in which the resulting improvement in sensitivity is of significant benefit. Therefore, the usefulness of the TDA in a limited number of receiver applications at X and K_u band as an RF pre- or postamplifier is expected to ultimately become negligible.

5) Mixer IF Amplifiers: Advances in Schottky-barrier mixer diode technology, first in Si and with even greater success in GaAs [6]–[10], has led to the evolution of the low-noise Schottky-diode mixer IF amplifier as the basic heterodyne downconverter in microwave and millimeter-wave front ends. Furthermore, coupling state-of-the-art mixer diodes with advanced circuit techniques, it is possible to configure simple mixer front ends which are competitive with more complex front ends employing RF preamplification, for both SSB and DSB reception, particularly in the millimeter-wave region up to 100 GHz.

The noise figure of this basic downconverter is essentially the product of the IF amplifier noise figure and the mixer conversion loss, be it SSB or DSB. The mixer conversion loss, in turn, is strongly dependent [28]–[34] upon the terminating impedances presented to the mixer diode(s) at the various higher order conversion products, e.g., idlers at frequencies $mf_{LO} \pm f_{IF}$, associated with a given IF (f_{IF}) and the mth order (m = 1,2,3,$\cdots$) harmonics of the LO (f_{LO}), particularly upon that at the image $f_i = 2f_{LO} - f_s$ corresponding to a given RF input signal f_s. In specific, the conventional matched-image (resistively terminated input over $f_{LO} \pm f_{IF}$) mixer in its various degrees of complexity (single ended, balanced, double balanced) is inherently a DSB converter providing equal conversion loss to RF inputs at f_s and f_i, e.g., $f_{LO} \pm f_{IF}$. It is therefore capable of exhibiting, in the state-of-the-art, impressively low DSB noise performance, particularly in the millimeter region (F_{DSB} = 3–7 dB over 1–100 GHz, assuming 1.5 dB F_{IF}), including the effects of circuit and diode losses on DSB conversion loss. The preceding results are dependent upon providing properly phased reactive terminations at said higher order idlers.

The implementation of the matched-image mixer for SSB reception (via a resistively isolated input preselector or a properly phased image-reject dual mixer configuration) degrades the preceding values by at least 3 dB. The matched-image mixer has the advantage, however, of half to full octave (or greater) bandwidth capability in both SSB and DSB applications. Practical cost-effective implementations of such Schottky-diode mixers, either in balanced or single-ended configurations, when integrated with a low-noise (1.5-dB) IF preamplifier, achieve SSB noise factors ranging from approximately 6 to 10 dB over the 1–100-GHz range [6], [35]–[37].

It has long been known [29]–[34] that proper reactive termination of the image frequency ($2f_{LO} - f_{RF}$) along with that of the higher order idlers can further reduce the conversion loss and noise factor of SSB downconverters by typically 1–2 dB. The advent of high-quality low-parasitic-content GaAs Schottky diodes has led to the practical realization of this potential in the image-enhanced and image-recovery mixer. The reactive image termination causes energy converted to the image frequency (only

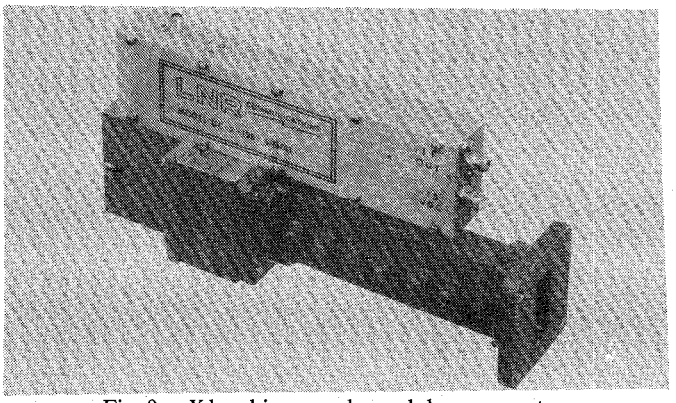

Fig. 9. *X*-band image-enhanced downconverter.

possible upon simultaneous properly phased reactive termination of the higher order idlers) to be reflected back into the mixer and reconverted to IF.

Reactive image termination is accomplished either by proper location of a signal frequency bandpass filter [31]–[33], [38], [39] at the signal input to a single-ended or balanced mixer, or by use of a unique image-recovery [40]–[43] configuration, incorporating a pair of identical constituent mixers with properly phased signal and LO inputs and IF output. These two image-enhancement techniques are associated with fixed LO, one-to-one RF to IF frequency translator and tunable LO, narrow-band IF modes of mixer operation.

The filter-type reactive image mixer, requires a fixed finite separation between the RF signal and image sidebands, and therefore generally utilizes wide-band IF's ranging from UHF to *S* band in order to minimize the signal frequency insertion loss of the input filter. Therefore, the practical implementation of reactive image termination mixers imposes a limitation on maximum achievable fractional signal circuit bandwidth of the order of 10 percent or less due to the narrow bandwidth restriction of a properly located filter in the signal input circuit to provide the required stopband reactive termination over the image band. However, in many communications applications, this bandwidth limitation can readily be accommodated so that many filter-type image-enhanced mixers integrated with low-noise transistor IF amplifiers have been implemented as practical hardware. A typical *X*-band mixer of this type is depicted in Fig. 9, wherein the waveguide input filter provides the reactive image termination, and the diode mount is designed to suppress the higher order idlers. The *X*-band unit shown exhibits a typical overall noise figure of 5 dB, while providing 40-dB image rejection.

The image-recovery mixer [40]–[43] depicted in Fig. 10 consists of a pair of balanced mixers coupled to a common input signal, LO and IF output ports through a lossless in-phase signal input network, a quadrature LO hybrid, and a quadrature IF output hybrid, respectively. This configuration provides a reactive image termination by virtue of its symmetry with the common signal junction appearing as a short circuit at the image. Typical measured performance of off-the-shelf mixers of this type are depicted along with best *X*-band laboratory results [34], [41] in Fig. 11.

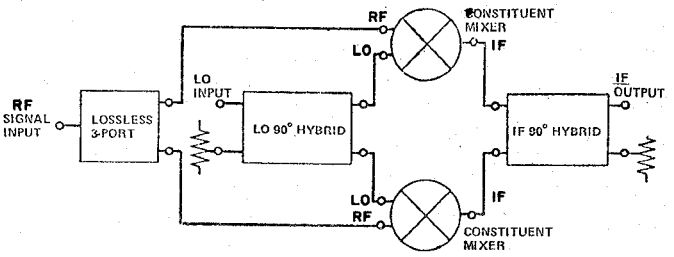

(a)

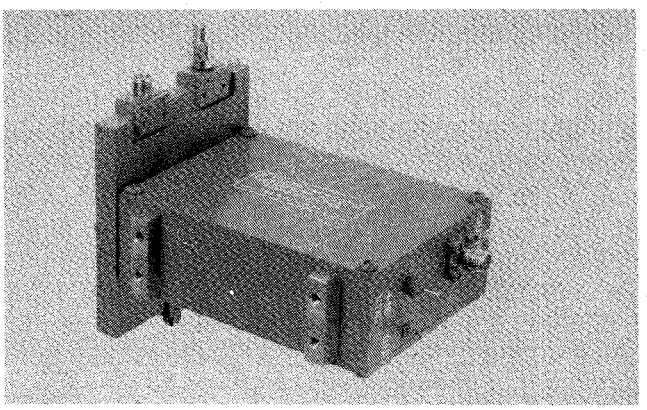

(b)

Fig. 10. Image-recovery mixer configuration. (a) Mixer block diagram. (b) Integrated mixer IF amplifier.

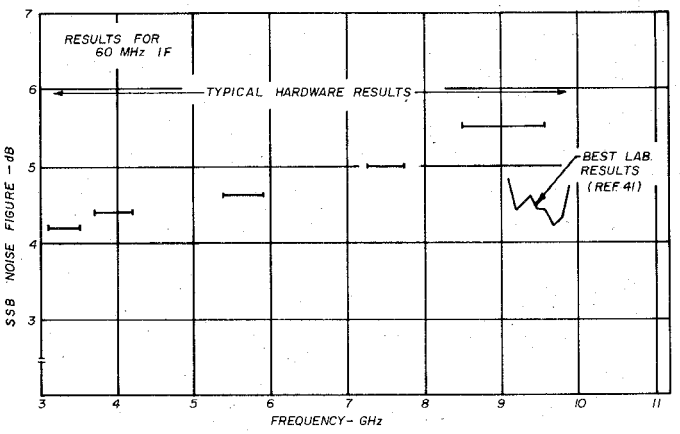

Fig. 11. Measured noise performance of image-recovery mixers.

More generally, the image-recovery technique, is applicable to low-frequency IF (30–70 MHz) and offers input RF bandwidths of 10 percent or greater and direct conversion front-end noise figures of 4–7 dB from *C* to *K* band. In both matched and reactive image mixer configurations, IM intercept points of 0–+20 dBm or better can be readily realized, simultaneously with low-noise performance. One can project further improvement in *both* SSB and DSB mixer IF amplifier noise performance and the consequent realization of competitive low-noise front ends without RF preamplification, particularly in the millimeter range, (F = 3–6 dB over 1–100 GHz) based upon the use of still higher quality, lower parasitic content Schottky diodes, the realization of computer-aided circuit design techniques for image enhancement over wider RF bandwidths, and the use of ultralow-noise *parametric* IF amplifiers ($F_{IF} \leq 1$ dB).

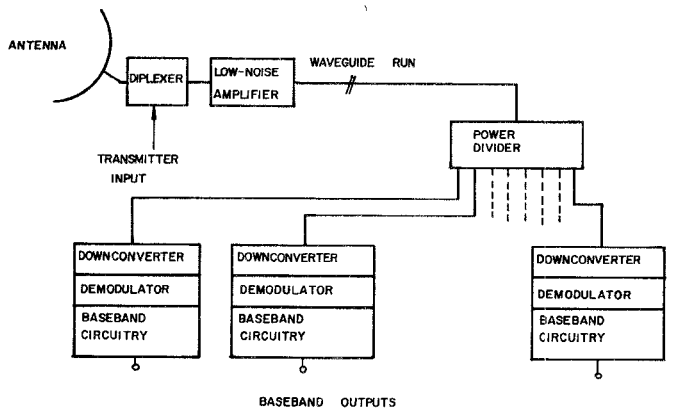

Fig. 12. Block diagram of satellite earth station receiving system.

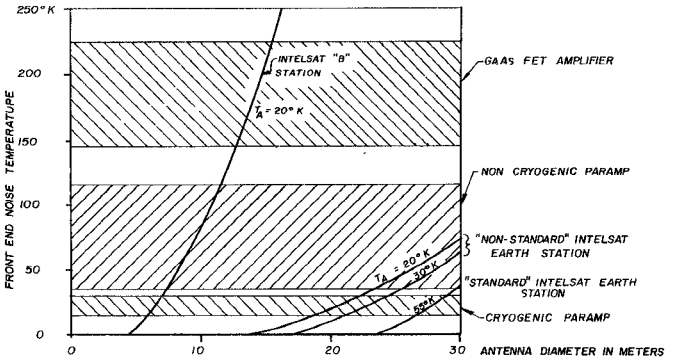

Fig. 13. Tradeoff between front-end noise temperature and antenna diameter for a 4-GHz INTELSAT earth station.

Still further improvement is achievable for operation of the mixer parametric IF amplifier at cryogenic temperatures [22] or in unique dual antiparallel diode subharmonically pumped [44]–[45] configurations.

IV. Importance of Receiver Noise Performance in Various System Applications

The need for state-of-the-art noise figure in microwave and millimeter-wave receiver applications arises for one of two reasons. In systems where front-end noise figure may be traded off against transmitter power and/or antenna size, the most economical system design often entails utilizing the lowest noise receiver available. In many applications system performance goals may only be achieved by utilizing the best available front end, antenna, and transmitter. These points are best illustrated with the following specific examples.

A. Satellite Communications

The demands of the satellite communications industry [6]–[8] have provided much of the impetus for the advancement in the low-noise art over the last decade, particularly in view of practical limitations on transmitter power and antenna size.

Other practical design considerations are as follows.

—SSB reception with image rejection is necessary to suppress interfering signals in the image passband.

—An input filter preceding the RF preamplifier or mixer is required to suppress out-of-band leakage from the system transmitter.

—High linear dynamic range is required to suppress intermodulation and cross modulation generated by time-coincident input signals and AM-to-PM conversion on strong signals.

—A high degree of amplitude flatness and phase linearity (delay flatness) in the receiver passband response is specified to prevent distortion of wide-band signals.

—Sufficiently high net RF/IF conversion gain to offset losses incurred in back-end multiplexing is necessary.

—RF bandwidth must be sufficiently large to permit multiple access.

—The IF bandwidth is chosen to accommodate wide-band FM signal modulation.

Fig. 12 shows a typical INTELSAT receiving system. The low-noise RF amplifier (LNA) comprises two paramp stages at the input, followed by three transistor stages, providing an overall gain of 55 dB. The transistor stages are biased for increasingly high dynamic range to minimize IM distortion and AM-to-PM conversion. The overall LNA gain is sufficient to reduce the noise temperature contribution of the following conventional power divider/downconverter array to less than 3 K. Use of more advanced mixers in the downconverter array to further reduce this contribution is less economical than increasing the gain of the LNA with relatively inexpensive bipolar transistor stages.

The figure of merit for a satellite receiving system [6]–[8] is G/T, which is the antenna gain divided by the system noise temperature T:

$$T = T_A + T_r = \frac{T_a}{L_F} + \left(1 + \frac{1}{L_F}\right) T_0 + T_r$$

where T_A is the equivalent antenna noise temperature, L_F is the feed loss, and T_r is the receiver noise temperature.

For a standard INTELSAT earth station,

$$G/T\,(\text{dB}) \geq 40.7 + 20 \log (f_{\text{GHz}}/4).$$

Fig. 13 shows the required receiver noise temperature, to provide the required G/T as a function of antenna diameter, with antenna noise temperature as a parameter, assuming antenna efficiency of 67 percent. Also shown is the requirement for an INTELSAT B earth station wherein the G/T may be 10 dB lower.

A standard INTELSAT station must provide the required G/T at elevation angles down to 5° above the horizon. Because the antenna temperature increases significantly at low angles, the G/T can only be met at this time with a cryogenic paramp. For a large number of INTELSAT stations, however, which are nonstandard and have a favorable elevation angle, noncryogenic paramps are used on the basis of their lower purchase and maintenance costs.

Due to the variations in predetection bandwidth and signal-to-noise requirements for acceptable link performance, the high G/T of a standard INTELSAT station is not always required. This opens up a wider range of tradeoffs in implementing small earth stations for specialized traffic. As described in the preceding section, there are three types of

low-noise amplifiers in use with various 4-GHz earth station receiving systems. These are cryogenic paramps, noncryogenic paramps (including units that are thermoelectrically cooled for the lowest noise, and lower cost designs that are temperature stabilized at the highest specified ambient), and GaAs FET amplifiers.

For the higher microwave satellite bands, there is a more diverse application of low-noise technology. For the 11.7–12.2-GHz CTS applications, the previously described (Fig. 8) Paraconverter® low-noise front end combines a single-stage advanced noncryogenic parametric amplifier, image-enhanced mixers, and low-noise microwave transistor IF amplifiers to provide a 200 K overall noise temperature in a housing that is directly mountable at the antenna feed. In this approach, the entire satellite band is translated to a lower microwave band, and conventional postreceivers are utilized for further downconversion and demodulation. The rapid strides in GaAs FET technology, the availability of low-noise mixer preamplifiers, and the lack of legal restriction on satellite radiated power will open a significant range of tradeoffs to system designers as the 11.7–12.2-GHz band is made available for commercial use. The choice will be made purely on the basis of economics. That is to say, the relative costs of satellite RF power, a tracking system for a highly directional earth station antenna, and a state-of-the-art low-noise parametric amplifier ($T_r < 100$ K) will have to be weighed.

As millimeter frequencies, through K_a band, the parametric amplifier is the sole practical choice, since limitations on satellite power, combined with high atmospheric attenuation, dictate the use of the lowest noise front end available.

B. Radar

Although state-of-the-art low-noise components find application in radar, they do so only in specialized applications.

Front-end noise figure enters into radar performance in two ways. The radar range equation [46] is

$$R_{\max} = k \cdot \left[\frac{P_t G^2}{S_{\min}}\right]^{1/4}$$

where $R_{\max}$ is the maximum range at which a target of given cross section can be detected, P_A is the peak transmitter power, G is the antenna gain expressed as a power ratio, and $S_{\min}$ is the minimum detectable signal (defined as the effective system input noise temperature).

The second way in which noise figure enters into radar performance is in parameter estimation such as angular location.

The theoretical angular accuracy of a radar is [46]

$$\delta\theta = \frac{0.628\theta_B}{(2S/N)^{1/2}}$$

where θ_B is the antenna beamwidth and S/N is the signal-to-noise ratio. Finally, improved receiving noise performance increases the probability of detection and decreases the false alarm rate. With all other parameters fixed, the signal-to-noise ratio varies inversely with the system noise temperature.

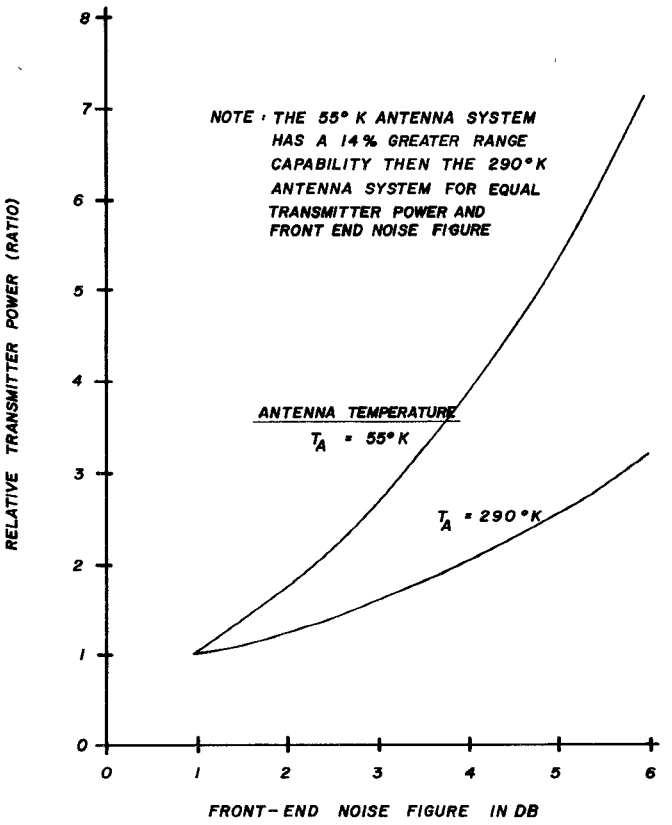

Fig. 14. Tradeoff between transmitter power and noise figure to achieve a given radar system range capability.

From these two equations it is seen that range increases with the fourth root of signal-to-noise, while angular accuracy varies as its square root. Moreover, it is seen that peak transmitter power can be directly traded off against system noise temperature. Fig. 14 shows this tradeoff for two antenna noise temperatures, 290 and 55 K. This plot shows relative transmitter power, to achieve a given range, versus front-end noise figure. A 290 K antenna noise temperature is typical of an air-to-ground radar, where the main beam illuminates the ground. In this case, it is generally more cost-effective to concentrate on maximizing transmitter power while utilizing a relatively low-cost conventional mixer preamp as the front-end noise-determining element. With the lower antenna temperature, as with a ground-to-air or air-to-air radar where the antenna "sees" the cold sky, a low-noise receiver can significantly enhance system performance.

Although the tradeoff between system noise temperature and transmitter power is important in a radar, the system performance can be more easily improved by increasing the antenna diameter. Therefore, state-of-the-art noise figure becomes important only when there is a constraint on antenna size, the latter due to location (for example, in an aircraft), to economics (as for a phased array), or to a requirement on a minimum width beam to achieve a required coverage (such as a cosecant-squared elevation pattern).

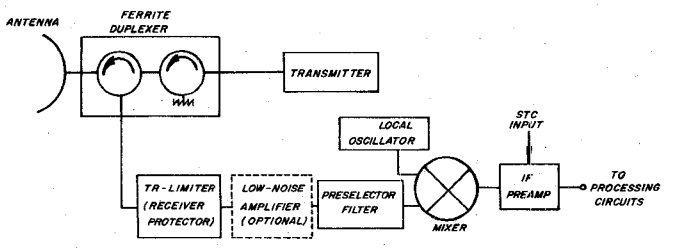

Fig. 15. Block diagram of a typical radar front-end.

Based upon the representative block diagram of Fig. 15, the practical design considerations for radar front ends include the following:

—Duplexer to separate transmitted and received signals.

—Input limiter preceding RF preamplifier or mixer to protect same from burnout during transmitter leakage pulse duration.

—Severe environmental requirements, including temperature, shock, vibration, etc.

—Phase and gain matching of front ends in sets of two or three for monopulse tracking radars.

—Size constraints for airborne systems.

—SSB reception with image rejection, often a desirable capability to minimize effects of interference in image band.

—High dynamic range of linear operation to inhibit large-signal distortion.

—High degree of amplitude flatness and phase linearity in the receiver passband response to minimize distortion in those systems using wide-band "chirped" FM pulses.

—Sufficiently wide RF bandwidth to accommodate system-derived requirement on transmitter carrier frequency diversity.

—Receiver blanking and/or sensitivity time control desirable to prevent overload during transmission, and from short-range returns.

Based upon the preceding section, the three low-noise front-end components that find application in radar front ends are parametric amplifiers, transistor amplifiers (bipolar and GaAs FET), and image-recovery mixers.

At X band and above, the image-recovery mixer (Figs. 10 and 11) has a number of advantages that make it particularly suitable for radar receivers, namely, its low-noise performance and its high dynamic range. The former eliminates the need for an RF amplifier with its additional size and weight, whereas the latter (1-dB-gain compression level at inputs greater than -15 dBm) eliminates the need for receiver desensitization circuitry at RF.

Below X band, improved system sensitivity can be obtained without excessive added size, weight, or cost by using a GaAs FET or bipolar transistor RF amplifier followed by a SSB mixer to avoid the contribution of image-band noise generated by the generally wide-band RF amplifier. Finally, in radar deployments where maximum receiver sensitivity is a necessity, a parametric RF amplifier must be used.

An example of the effects of X-band front-end noise figure on radar range capability, presented graphically in Fig. 16, summarizes the impact of low-noise receiver technology on radar performance.

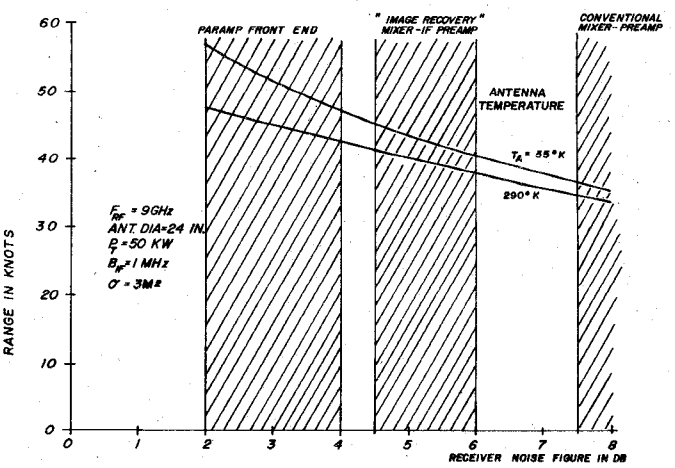

Fig. 16. Range capability versus noise figure for typical X-band radar parameters.

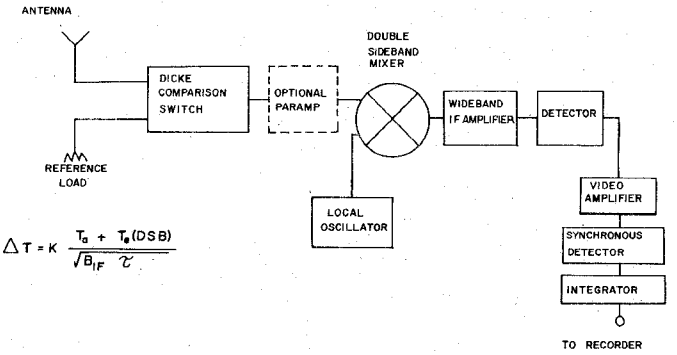

Fig. 17. Block diagram of a radiometric receiver.

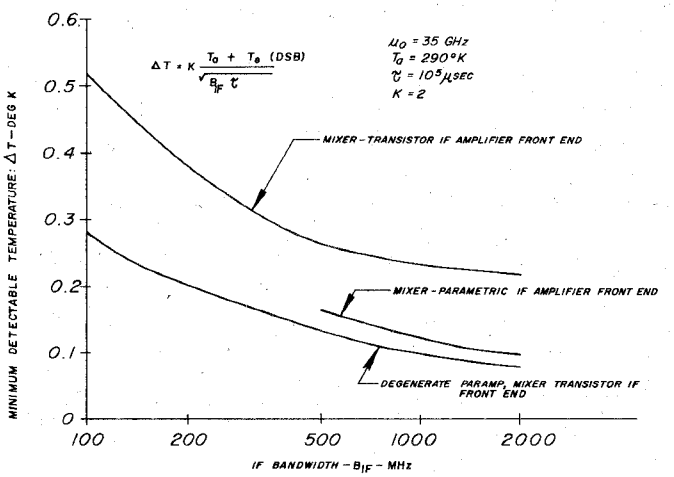

Fig. 18. Sensitivity of alternative K_a-band radiometric receivers.

C. Radiometric Receivers

Radiometric receivers find use both in radio astronomy and in certain mapping and guidance systems. Fig. 17 depicts a typical radiometric receiver, and Fig. 18 formulates its sensitivity in terms of minimum detectable temperature, that is, the change in receiver-input broad-band noise temperature level that produces a change in detector output

equal in amplitude to the internally generated rms fluctuation. Shown in Fig. 18 are the key radiometer parameters and their relation to sensitivity.

Radiometric receivers may be located in a relatively controlled stable environment for radio astronomy, or may be required to meet full military environmental specifications for airborne mapping or guidance applications. This can significantly affect the choice of front-end components. Other key constraints [21] are the following:

—DSB reception to maximize ability to detect low-level broad-band noise spectra.

—Utilization of Dicke configuration including square-wave-driven switch and synchronous detector, the former alternately connecting the receiver input to the receiving antenna and a reference load and thereby reducing the effects of short-term variation in receiver gain and noise temperature stability.

—Sufficiently large IF (predetection) bandwidth to enhance the radiometer detection sensitivity.

—Sufficiently large RF bandwidth to include both sidebands of width B_{IF}.

To illustrate the tradeoffs available in radiometric receiver design [21] based upon the previously presented (Fig. 3) building block state-of-the-art, the sensitivity of the following three alternative 35-GHz front ends is presented as a function of IF bandwidth in Fig. 18:

—A degenerate paramp followed by a mixer and transistor IF amplifier.

—A mixer and transistor IF amplifier.

—A mixer and a parametric IF amplifier.

Fig. 18 illustrates a key point relative to the millimeter-wave front-end state-of-the-art. Above 40 GHz, the judicious use of advanced mixer technology, including cryogenic cooling, can result in the realization of a comparable or lower noise front end than with a millimeter paramp, due to practical limitations on pump frequency and varactor cutoff which limit the noise figure achievable with millimeter paramps.

V. Future Trends in Low-Noise Receivers

Based upon the preceding assessment of the current state-of-the-art in microwave and millimeter front ends, one may project the following trends.

—Evolutionary improvements in GaAs technology toward highly reliable, extremely small metal semiconductor (MES) configurations will extend the frequency range of all devices.

—The noncryogenic parametric amplifier will continue to provide the lowest noise performance in a cost-effective reliable front end because of its basically noise-free amplification mechanism. Cryogenic paramps will only be used where the ultimate in noise-free reception is required. The predominant paramp applications will be in satellite communications ground station receivers.

—MESFET devices will play an increasingly important role, through X band, as RF preamplifiers and postamplifiers for parametric RF preamplifiers, as well as microwave IF amplifiers. MESFET RF preamplifiers will play an increasingly dominant role in small earth station point-to-point communications receivers as well as radar receivers.

—For many moderately low-noise receiver applications, particularly in the millimeter-wave radar and radiometric region, simple front ends consisting of ultralow-loss Schottky-barrier mixers followed by ultralow-noise transistor or parametric IF amplifiers will eliminate the need for RF preamplification. A particularly useful application for this configuration is in millimeter radio astronomy installations.

In each case, advances in the receiver art will be ultimately linked to further concurrent advances not only in semiconductor device technology but in related areas such as ferrite circulator technology, advanced planar, and mixed media transmission line techniques and circuit and structural design concepts.

Acknowledgment

The authors wish to thank Dr. F. Arams and S. Okwit, P. Lombardo, W. Hollis, and J. DeGruyl for their contributions in the preparation of this paper.

References

[1] R. Adler *et al.*, "Description of the noise performance of amplifiers and receiving systems," *Proc. IEEE*, vol. 51, pp. 436–442, Mar. 1963.
[2] H. C. Okean and P. P. Lombardo, "Noise performance of M/W and MM-wave receivers," *Microwave J.*, pp. 41–50, Jan. 1973.
[3] D. C. Hogg and W. W. Mumford, "The effective noise temperature of the sky," *Microwave J.*, vol. III, pp. 80–85, Mar. 1960.
[4] G. L. Heiter, "Characterization of nonlinearities in microwave devices and systems," *IEEE Trans. Microwave Theory Tech.*, vol. MTT-21, pp. 797–805, Dec. 1973.
[5] D. E. Norton, "The cascading of high dynamic range systems," *Microwave J.*, pp. 57–71, June 1973.
[6] C. L. Cuccia, "Status report: Modern low noise amplifiers in communications systems," *Microwave Syst. News*, pp. 120–132, Aug./Sept. 1974, and pp. 79–89, Oct./Nov. 1974.
[7] C. L. Cuccia and C. Hellman, "The low-cost low-capacity earth terminal," *Microwave Syst. News*, pp. 19–42 June/July 1975.
[8] C. L. Cuccia and C. Hellman, "Status report: Microwave communications update—1976," *Microwave Syst. News*, pp. 20–53, Feb./Mar. 1976.
[9] F. R. Arams *et al.*, "State-of-art low noise receivers for microwave and millimeter communications," to be presented at National Telecommunications Conference, Dallas, TX, Nov. 1976.
[10] W. Hollis, "Practical state-of-the-art of microwave and millimeter wave receiver front ends," *Commun. News*, Oct. 1976.
[11] J. Edrich, "20°K-cooled parametric amplifier for 46 GHz with less than 60°K noise temperature," *1973 IEEE—G-MTT Int. Symp. Digest*, pp. 72–74, June 1973.
[12] H. C. Okean, J. A. DeGruyl, and E. Ng, "Ultra low noise K_a-band parametric amplifier assembly," *1976 IEEE S-MTT Int. Microwave Symp. Digest*, pp. 82–84, June 1976.
[13] E. Kraemer, J. Leeper, and J. Whelehan, "K_u-band spacecraft parametric amplifier," *1974 IEEE S-MTT Int. Symp. Digest*, pp. 222–224, June 1974.
[14] A. D'Ambrosio, "A SHF parametric amplifier for space applications: Design implementation," *Alta Frequenza*, vol. XLIII, pp. 876–883, 1974.
[15] H. C. Okean *et al.*, "Electronically-tunable, low noise K_a-band paramp—downconverter satellite communications receiver," *1975 IEEE S-MTT Int. Microwave Symp. Digest*, pp. 43–45, May 1975.
[16] J. Whelehan *et al.*, "A nondegenerate millimeter wave parametric amplifier with a solid-state pump source," *1973 IEEE G-MTT Int. Symp. Digest*, pp. 75–77, June 1973.
[17] H. C. Okean, J. R. Asmus, and L. J. Steffek, "Low noise 94 GHz parametric amplifier development," *1973 IEEE G-MTT Int. Microwave Symp. Digest*, pp. 78–79, June 1973.
[18] H. C. Okean and L. J. Steffek, "Low loss, 3MM junction circulator," *1973 IEEE G-MTT Int. Microwave Symp. Digest*, pp. 80–81, June 1973.
[19] S. D. Lacey, B. T. Hughes, and J. C. Vokes, "A low noise room

temperature 12 GHz parametric amplifier," *1974 IEEE S-MTT Int. Symp. Digest*, pp. 220–221, June 1974.
[20] T. Okajima *et al.*, "18 GHz paramps with triple-tuned gain characteristics," *IEEE Trans. Microwave Theory Tech.*, vol. MTT-20, pp. 812–819, Dec. 1972.
[21] LNR Staff, "Millimeter wave radiometric sensitivity," *Microwave J.*, pp. 56–57, Jan. 1973.
[22] S. Weinreb and A. R. Kerr, "Cryogenic cooling of mixers for millimeter and centimeter wavelengths," *IEEE J. Solid-State Circuits*, pp. 58–63, Feb. 1973.
[23] C. A. Liechti and R. L. Tillman, "Design and performance of microwave amplifiers with GaAs Schottky gate field effect transistors," *IEEE Trans. Microwave Theory Tech.*, vol. MTT-22, pp. 510–517, May 1974.
[24] N. K. Osbrink *et al.*, "Transistor technology at microwave frequencies," *Microwave J.*, pp. 27–29, Nov. 1975.
[25] J. T. Lindauer and N. K. Osbrink, "GaAs FET amplifiers are closing fast on the low-noise narrow band leaders," *Microwave Syst. News*, pp. 63–67, May 1976.
[26] M. G. Walker *et al.*, "MESFET amplifiers go to 18 GHz," *Microwave Syst. News*, pp. 39–48, May 1976.
[27] H. C. Okean, "Tunnel diodes," ch. 8 in *Semiconductors and Semimetals*, vol. 7B, Willardson and Beer, Eds. New York: Academic Press, 1971.
[28] H. C. Torrey and C. A. Whitmer, "Crystal rectifiers," *Rad. Lab. Series*, vol. 15. New York: McGraw-Hill, 1948.
[29] R. J. Mohr and S. Okwit, "A note on the optimum source conductance of crystal mixers," *IRE Trans. Microwave Theory Tech.*, vol. MTT-8, pp. 662–627, Nov. 1960.
[30] A. A. M. Saleh, *Theory of Resistive Mixers*, The M.I.T. Press, 1971.
[31] S. Egami, "Nonlinear, linear analysis and computer-aided design of resistive mixers," *IEEE Trans. Microwave Theory Tech.*, vol. MTT-21, pp. 270–275, Mar. 1973.
[32] M. R. Barber, "Noise figure and conversion loss of the Schottky barrier mixer diode," *IEEE Trans. Microwave Theory Tech.*, vol. MTT-15, pp. 629–635, Nov. 1967.
[33] G. B. Stracca, F. Aspesi, and T. D'Angelo, "Low noise microwave down-converter with optimum matching at idle frequencies," *IEEE Trans. Microwave Theory Tech.*, vol. MTT-21, Aug. 1973.
[34] A. J. Kelly, H. C. Okean, and S. J. Foti, "Low noise microwave and millimeter wave integrated circuit mixers," *IEEE S-MTT Int. Microwave Symp. Digest*, pp. 146–148, May 1975.
[35] L. T. Yuan, "A low noise broadband K_a-band waveguide mixer," *IEEE S-MTT Int. Microwave Symp. Digest*, pp. 272–273, May 1975.
[36] T. G. Phillips and K. B. Jefferts, "Millimeter wave receivers and their application to radio astronomy," *1974 IEEE S-MTT Int. Microwave Symp. Digest*, pp. 116–117, June 1974.
[37] M. V. Schneider and G. T. Wrixon, "Development and testing of a receiver at 230 GHz," *1974 IEEE S-MTT Int. Microwave Symp. Digest*, pp. 120–122, June 1974.
[38] L. E. Dickens and D. W. Maki, "An integrated circuit balanced mixer, image and sum enhanced," *IEEE Trans. Microwave Theory Tech.*, vol. MTT-23, pp. 276–281, Mar. 1975.
[39] Y. Konishi, K. Uenakada, N. Yazawa, N. Hoshino, and T. Takahashi, "Simplified 12-GHz low-noise converter with mounted planar circuit in waveguide," *IEEE Trans. Microwave Theory Tech.*, vol. MTT-22, pp. 451–455, Apr. 1974.
[40] T. H. Oxley, J. F. Lord, K. J. Ming, and J. Clarke, "Image recovery mixers," *Proceedings 1971 European Microwave Conf.*
[41] A. J. Kelly and H. C. Okean, "Wideband image recovery mixers," *1974 GOMAC Digest of Papers*, pp. 240–241, June 1974.
[42] D. Neuf, "A quiet mixer," *Microwave J.*, vol. 16, pp. 29–32, May 1973.
[43] L. E. Dickens and D. W. Maki, "A new 'phased-type' image enhancement mixer," *1975 IEEE S-MTT Int. Microwave Symp. Digest*, pp. 149–151.
[44] M. V. Schneider and W. W. Snell, Jr., "Harmonically pumped strip line downconverter," *IEEE Trans. Microwave Theory Tech.*, vol. MTT-23, pp. 271–275, Mar. 1975.
[45] M. Cohn *et al.*, "Harmonic mixing with an antiparallel diode pair," *IEEE Trans. Microwave Theory Tech.*, vol. MTT-23, pp. 667–673, Aug. 1975.
[46] M. I. Skolnik, *Introduction to Radar Systems*. New York: McGraw-Hill, 1962.